Supporting Information

Shi et al. 10.1073/pnas.1119738109

SI Text

To verify that transcription factor A (TFAM) induces structural changes in DNA, we used FRET experiments. We incorporated the fluorescent cytosine analog tC^O (1) at several positions close to the heavy-strand promotor 1 (HSP1) transcription initiation site in both the template (sequences D3 and D4) and sense (sequences D1 and D2) strand (sequences in Table S1). We also synthesized the corresponding complementary oligonucleotides (natural sequences N1 and N2), including some sequences in which one cytosine was replaced by the nonemissive cytosine analog tC_{nitro} (2), which functions as a FRET acceptor for tC^O (sequences A1–A4; Table S1, emission/absorption spectra for tC^O–tC_{nitro} showing the energy overlap determining the J-integral are presented in Fig. S1). The FRET-pair facilitates detailed studies of variations in both distance and orientation within DNA duplexes using changes in donor (tC^O) emission/fluorescence lifetime (3).

First, we used four different DNA duplexes containing the FRET-pair tC^O–tC_{nitro} (D1–A1; D2–A2; D3–A3, and D4–A4; Table S1). The probes were incorporated at various positions, framing the transcription start site over six base pairs. FRET efficiencies for all four duplexes (17–21%; Table S2, representative spectrum shown in Fig. S1) are very similar to values that have been experimentally (using fluorescence lifetimes of tC^O) and theoretically determined previously for this relative distance and orientation of tC^O–tC_{nitro} in a B-DNA helix ($E_{FRET,\,experiment}$ = 20%, $E_{FRET,\,theory}$ = 18%) (3). The measured values therefore confirmed the integrity of the duplexes and the correct positioning of the probes. The tiny variations observed could be explained by differences in the local sequence surrounding the probe. Next, TFAM was added to these four duplexes, resulting in an increase in the efficiency of energy transfer from tC^O to tC_{nitro} between 8.3% and 15% (Table S2) and confirming that the binding of TFAM induces significant structural changes in the template that could be consistent with DNA breathing. In a duplex system designed to have a seven-base mismatch bubble over the transcription start site, we find a FRET efficiency of 65% (Table S2, D4–A_{BUB}). Compared with the 29% we get for the corresponding base-paired duplex with TFAM bound to it, this FRET efficiency suggests that the structural change upon TFAM binding is large, maybe corresponding to a premelted region, however, not as large as a 7 base mismatch bubble. The effect was, however, not dependent on the high-affinity TFAM binding site located immediately upstream of HSP, but rather a consequence of TFAM's ability to bind and bend any DNA sequence, because similar changes in FRET efficiency were seen using a template lacking the high-affinity TFAM site (Tables S1 and S2, duplex D_{MUT}–A_{MUT}).

SI Materials and Methods

FRET Measurements. Duplexes were prepared at a concentration of 2 μM in Tris·HCl buffer (pH 7.5; 20 mM Tris, 10 mM Mg^{2+}). Concentrations were set by recording the absorption at 260 nm. The extinction coefficients of the various sequences were calculated as the linear combination of the extinction coefficients of the individual bases (including tC^O and tC_{nitro}). This sum was multiplied by 0.9 to correct for base-stacking interactions. The values for the extinction coefficients that were used for the different bases at 260 nm were ε_T = 9,300 $M^{-1}\cdot cm^{-1}$, ε_C = 7,400 $M^{-1}\cdot cm^{-1}$, ε_G = 11,800 $M^{-1}\cdot cm^{-1}$, ε_A = 15,300 $M^{-1}\cdot cm^{-1}$, $\varepsilon_{tC_{nitro}}$ = 10,700 $M^{-1}\cdot cm^{-1}$, and ε_{tC^O} = 11,000 $M^{-1}\cdot cm^{-1}$. Calculating as described above yielded the following absorption coefficients of the sequences listed in Table S1: $\varepsilon_{D1} = \varepsilon_{D2}$ = 670,950 $M^{-1}\cdot cm^{-1}$, $\varepsilon_{D3} = \varepsilon_{D4}$ = 686,070 $M^{-1}\cdot cm^{-1}$, $\varepsilon_{A1} = \varepsilon_{A2}$ = 685,800 $M^{-1}\cdot cm^{-1}$, $\varepsilon_{A3} = \varepsilon_{A4}$ = 670,680 $M^{-1}\cdot cm^{-1}$, ε_{N1} = 682,830 $M^{-1}\cdot cm^{-1}$, ε_{N2} = 667,710 $M^{-1}\cdot cm^{-1}$, ε_{DMUT} = 701,640 $M^{-1}\cdot cm^{-1}$, ε_{AMUT} = 669,690 $M^{-1}\cdot cm^{-1}$, ε_{NMUT} = 666,720 $M^{-1}\cdot cm^{-1}$, and ε_{ABUB} = 655,920 $M^{-1}\cdot cm^{-1}$. DNA duplexes were prepared by mixing equal volumes of 4-μM samples of the tC^O sequences with 4.6-μM samples of the complementary natural sequences or those containing tC_{nitro}. A 15% excess of the latter sequences was used to ensure full hybridization of all sequences containing tC^O. Next, the samples were annealed by heating from room temperature to 95 °C over 10 min, keeping the temperature at 95 °C for 5 min, followed by slow cooling to 5.5 °C over 12 h. Hereafter, 1 mM DTT, 1 mM ATP (and Tris·HCl buffer) were added to the samples, reducing the duplex concentration to 1.64 μM (or 0.89 μM) in Tris·HCl buffer (pH 7.5; 18 mM Tris, 9 mM Mg^{2+}). Furthermore, appropriate volumes of the protein TFAM (stock: 60 μM in 20 mM Tris, 800 mM NaCl) or its corresponding buffer were added, leading to further alterations in the duplex and ion concentration of the samples, which resulted in final ratios of proteins to DNA duplex as indicated in Table S2. After addition of TFAM, samples were incubated for 10 min.

FRET efficiencies were determined using the average lifetime of tC^O in the various duplexes as follows:

$$E_{FRET} = 1 - \frac{<\tau_{DA}>}{<\tau_D>},$$

where $<\tau_{DA}>$ and $<\tau_D>$ denote the average fluorescence lifetime of the donor in the presence and absence of the acceptor, respectively, and where

$$<\tau> = \frac{\sum A_i\tau_i}{\sum A_i},$$

with A_i being the amplitude corresponding to τ_i.

Lifetimes were recorded using time-correlated single-photon counting. A PicoQuant LDH-P-C-375 pulsed diode with an approximate center wavelength of 375 nm was used as an excitation source at a repetition rate of 10 MHz. All measurements were performed at room temperature. Decays were recorded at an emission wavelength of 460 nm in a time window of 100 ns with the spectral resolution of the monochromator set to 10 nm. Photons were collected by a microchannel-plate photomultiplier tube (MCP-PMT R3809U-50; Hamamatsu) and fed into a multichannel analyzer with 2,048 channels. A minimum of 10,000 counts were recorded in the top channel. The intensity decays were convoluted with the instrument response function, which had a FWHF of ~100 ps, and fitted to two or three exponential expressions with the software FluoFit (PicoQuant; χ^2 ranging from 0.84 to 1.26). For all samples, one lifetime (~12 ns) originated from a contamination (maximum ~5% amplitude weighted) and was therefore not taken into account for calculations of the average lifetimes. This contamination was also present in single-stranded samples, and its extent varied between sequences, proving that it is not due to artifacts upon duplex formation or protein interactions. Most measurements were repeated for three independent samples, resulting in the presented SDs.

Expression and Purification of Topoisomerase I. Mitochondrial topoisomerase I (TOP1mt) was expressed from recombinant baculoviruses. After infection, Sf9 cells were grown in suspension

and collected after 60–72 h. The infected cells were frozen in liquid nitrogen and thawed at 4 °C in lysis buffer containing 25 mM Tris·HCl (pH 8.0), 10 mM 2-mercaptoethanol, and 1× protease inhibitors (100× stock of protease inhibitors contained 100 mM phenylmethylsulfonyl fluoride, 200 mM pepstatin A, 60 mM leupeptin, and 200 mM benzamidine in 100% ethanol) and incubated on ice for 20 min before the cells were transferred to a Dounce homogenizer and lysed by 20 strokes of a tight-fitting pestle. NaCl was added to a final concentration of 0.8 M, and the homogenate was swirled gently for 40 min at 4 °C before cleared by centrifugation at 45,000 rpm for 45 min at 4 °C using a Beckman TLA 100.3 rotor. The TOP1mt extract was diluted 1:1 with buffer A [25 mM Tris·HCl (pH 8.0), 10% (vol/vol) glycerol, 1× protease inhibitors, and 10 mM 2-mercaptoethanol] containing 20 mM imidazole. Ni^{2+}-NTA matrix superflow (APBiotech) was pre-equilibrated in buffer A containing 10 mM imidazole, and 2 mL of the resin was added to the extract and incubated with gentle rotation at 4 °C for 40 min. The Ni^{2+}-NTA resin was collected by centrifugation (1,500 × *g*, 10 min, 4 °C), resuspended in buffer A (40 mM imidazole, 0.4 M NaCl), poured into a column, and washed with 10-column volumes of the same buffer, followed by elution with buffer A (250 mM imidazole, 0.4 M NaCl). The buffer was exchanged to buffer C [50 mM NaPO4 (pH 7.0), 10% (vol/vol) glycerol, 1 mM DTT, protease inhibitors, 0.5 mM EDTA] supplemented with 0.1 M NaCl. Recombinant TOP1mt was loaded on a 1-mL HiTrap heparin column (APBiotech) equilibrated in buffer C (0.1 M NaCl). After washing with three-column volumes of buffer C (0.1 M NaCl), the protein was eluted with a linear gradient (10 mL) of buffer C (0.1–1.5 M NaCl). TOP1mt was eluted at ∼1.1 M NaCl. The peak fractions were diluted 10× with buffer C (0 M NaCl) and loaded on a 1-mL HiTrap SP column (APBiotech) equilibrated in buffer C (0.1 M NaCl). After washing with three-column volumes of buffer C (0.1 M NaCl), TOP1mt was eluted with linear gradient (10 mL) of buffer C (0.1–1.5 M). TOP1mt was eluted at 0.7 M NaCl. The yield of TOP1mt from 400 mL of culture was 2 mg. The purity of the protein was at least 95% as estimated by SDS/PAGE and Coomassie blue staining.

1. Sandin P, et al. (2008) Characterization and use of an unprecedentedly bright and structurally non-perturbing fluorescent DNA base analogue. *Nucleic Acids Res* 36: 157–167.
2. Preus S, Börjesson K, Kilså K, Albinsson B, Wilhelmsson LM (2010) Characterization of nucleobase analogue FRET acceptor tCnitro. *J Phys Chem B* 114:1050–1056.
3. Börjesson K, et al. (2009) Nucleic acid base analog FRET-pair facilitating detailed structural measurements in nucleic acid containing systems. *J Am Chem Soc* 131: 4288–4293.

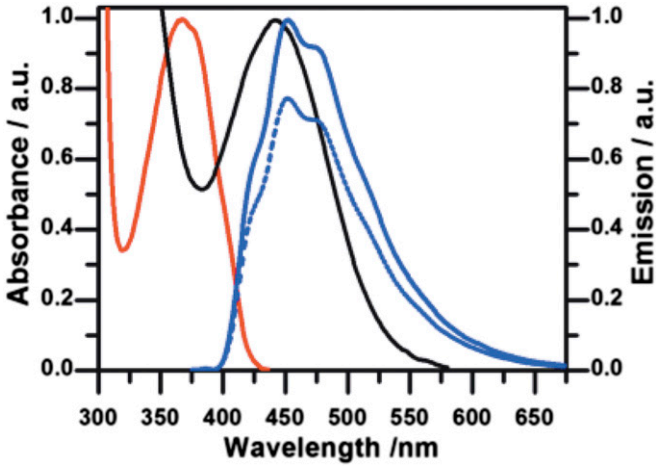

Fig. S1. Representative absorption spectra of the cytosine analogs tC^{O} (red) and tC_{nitro} (black) in DNA context. Emission spectra of tCO in duplex D1–N1 (without FRET acceptor tC_{nitro}; blue solid line) and in D1–A1 (with acceptor tC_{nitro} at 6-bp distance; blue dotted line), illustrating the overlap with tCnitro absorption.

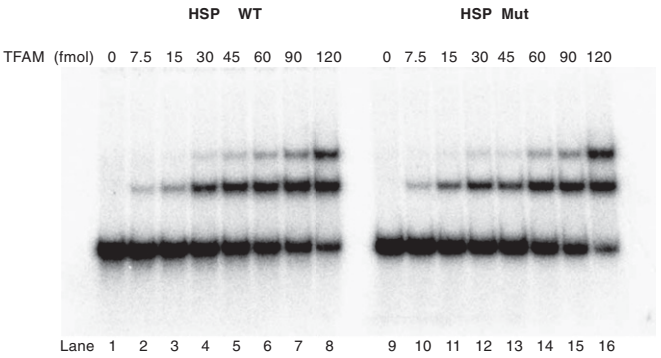

Fig. S2. TFAM binds efficiently to DNA both in the absence and presence of the TFAM binding site. A 64-bp–long DNA fragment (30 fmol) corresponding to human HSP1 (from position −42 to +22 relative the transcription start site) was used to monitor TFAM binding. For comparison, we used a similar DNA fragment, but mutated the TFAM binding site at position −26 to −35 relative to the HSP transcription start site by changing A to C, C to A, T to G, and G to T (the sequence is indicated in Fig. 1*A*). As demonstrated in Fig. 1*D*, this mutation completely abolishes TFAM-dependent transcription. We incubated the WT and mutant DNA fragments with increasing amounts of TFAM (from 0 to 120 fmol TFAM, as indicated in the figure). Two distinct bands were observed, most likely corresponding to one or two TFAM monomers binding to the same DNA fragment. The reaction conditions were 20 mM Tris·Cl (pH 8.0), 10 mM MgCl2, 1 mM DTT, 100 μg/mL BSA, and 40 mM NaCl. The samples were incubated at 32 °C for 15 min, separated on a 6% (wt/vol) nondenaturing PAGE gel, and visualized by PhosphorImager.

Table S1. DNA sequences containing the FRET-pair consisting of fluorescent cytosine analog tC^O (X) as a donor (D) and nonemissive cytosine analog tC_{nitro} (Y) as an acceptor (A)

DNA sequence	Sequence name
5′-d(CAGCACACACACACCGCTGCTAACCCCATACCCCGAACCAACCAAA**X**CCCAAAGGCACCCCCCACAGTTT)-3′	D1
3′-d(GTCGTGTGTGTGTGGCGACGATTGGGGTATGGGGCTTGGTTGGTTTGGGGTTT**Y**CGTGGGGGGTGTCAAA)-5′	A1
5′-d(CAGCACACACACACCGCTGCTAACCCCATACCCCGAACCAACCAAAC**X**CCAAAGGCACCCCCCACAGTTT)-3′	D2
3′-d(GTCGTGTGTGTGTGGCGACGATTGGGGTATGGGGCTTGGTTGGTTTGGGGTTTC**Y**GTGGGGGGTGTCAAA)-5′	A2
3′-d(GTCGTGTGTGTGTGGCGACGATTGGGGTATGGGGCTTGGTTGGTTTGGGGTTTCCGTGGGGGGTGTCAAA)-5′	N1
5′-d(CAGCACACA*ACACAATAGTAGCCAAAACGC*CCCCGAACCAACCAAA**X**CCCAAAGGCACCCCCCACAGTTT)-3′	D_{MUT}
3′-d(GTCGTGTGT*TGTGTTATCATCGGTTTTGCG*GGGGCTTGGTTGGTTTGGGGTTT**Y**CGTGGGGGGTGTCAAA)-5′	A_{MUT}
3′-d(GTCGTGTGT*TGTGTTATCATCGGTTTTGCG*GGGGCTTGGTTGGTTTGGGGTTTCCGTGGGGGGTGTCAAA)-5′	N_{MUT}
5′-d(AAACTGTGGGGGGTG**X**CTTTGGGGTTTGGTTGGTTCGGGGTATGGGGTTAGCAGCGGTGTGTGTGCTG)-3′	D3
3′-d(TTTGACACCCCCCACGGAAACC**Y**CAAACCAACCAAGCCCCATACCCCAATCGTCGCCACACACACACGAC)-5′	A3
5′-d(AAACTGTGGGGGGTGC**X**TTTGGGGTTTGGTTGGTTCGGGGTATGGGGTTAGCAGCGGTGTGTGTGCTG)-3′	D4
3′-d(TTTGACACCCCCCACGGAAACCC**Y**AAACCAACCAAGCCCCATACCCCAATCGTCGCCACACACACACGAC)-5′	A4
3′-d(TTTGACACCCCCCACGGAAACCCCAAACCAACCAAGCCCCATACCCCAATCGTCGCCACACACACACGAC)-5′	N2
3′-d(TTTGACACCCCCCACG*CCCCTAT***Y**AAACCAACCAAGCCCCATACCCCAATCGTCGCCACACACACACGAC)-5′	A_{BUB}

Corresponding unmodified natural sequences are also shown (labelled N1, N_{MUT}, and N2 in the table). The high-affinity TFAM binding site is underlined and the transcription start site is highlighted in gray. Mutations to the original sequence are shown in italic.

Table S2. Energy-transfer efficiencies of the tC^O–tC_{nitro} FRET-pair in four different WT duplexes, a duplex with mutated TFAM binding site (D_{MUT}–A_{MUT}), and a duplex containing a 7-bp bubble over the transcription start site (D4–A_{BUB}) (E_{FRET})

DNA duplex*	E_{FRET}, %	$E_{FRET, TFAM}$, %†	ΔE_{FRET}, %
D1–A1	21 ± 0.2	31 ± 0.1	10 ± 0.2
D2–A2	17 ± 0.3	29 ± 0.4	12 ± 0.5
D3–A3	17 ± 0.3	32 ± 0.8	15 ± 0.9
D4–A4	21 ± 0.4	29 ± 0.4	8.3 ± 0.6
D_{MUT}–A_{MUT}	21 ± 0.2	30 ± 0.8	10 ± 0.8
D4–A_{BUB}	65 ± 0.06		44 ± 0.4‡

FRET efficiencies in the presence of TFAM ($E_{FRET, TFAM}$) as well as the corresponding change in FRET efficiencies (ΔE_{FRET}) are also listed. Error intervals show the SD.

*Full sequences are listed in Table S1.

†Samples containing a ratio of 3:1 TFAM:DNA.

‡$\Delta E_{FRET} = E_{FRET, D4–ABUB} - E_{FRET, D4–A4}$.